

Process optimisation of PA11 in fiber-laser powder-bed fusion through loading of an optical absorber

Christian Leslie Budden*¹, Aakil Raj Lalwani^{1,3}, Kenneth Ælkær Meinert¹,
Anders Egede Daugaard² & David Bue Pedersen¹

¹Department of Mechanical and Civil Engineering, Technical University of Denmark,
Kgs. Lyngby, Denmark

²Danish Polymer Centre, Department of Chemical and Biochemical Engineering,
Technical University of Denmark, Kgs. Lyngby, Denmark

³LEGO System A/S, Billund, Denmark

*Corresponding author: clebu@mek.dtu.dk

Abstract

Industrial laser processing is rapidly shifting towards fiber lasers with wavelengths between 780nm and 2200nm. This can be largely contributed to the excellent beam properties and, ease of operation. However, for Additive Manufacturing of polymers, CO₂ lasers at wavelengths of 10,6µm are predominantly used. CO₂ lasers provide unmatched energy absorption by the C-H bonds of Polyamide (PA). To remedy this, the current study investigates using a high-power fiber laser (1080nm) for consolidating PA11 mixed with a black optical absorber. Several compositions are produced by mixing commercially available white and black powder. Aiming at finding the optimum optical absorber loading and the corresponding process parameters, allowing the highest possible component fidelity, while achieving the lightest hue of grey possible to allow for later colouring. The experiment is conducted on an in-house developed Open Architecture Laser Powder-Bed Fusion system. The parts are examined through, surface roughness, and mechanical characterisation.

Introduction

Laser Powder Bed Fusion (L-PBF) is rapidly increasing its popularity in industry. Several materials can be used in the process, with the most predominant materials being polymers, metals, and ceramics. Typically, polymer sintering machines use a CO₂ laser, because polymer bonds react to the wavelength of the laser, leading to heating, sintering, and melting of the polymer [1].

Commercial polymer L-PBF systems like that of EOS and 3DSystems are equipped with CO₂ lasers. However, two main limiting factors in terms of the resolution are the layer thickness (vertical) and the laser beam spot size (lateral). A fiber laser source holds certain advantages over a CO₂ laser. Such as a gaussian beam profile, and a high-power laser, while being a cost-effective solution. Furthermore, the beam delivery system into the scanner via fiber allows for a finer beam spot size, which helps improve the lateral resolution. Another advantage of a fiber laser is the high stability and good beam profile achieved during pulsing. These effects are utilised in the Open Architecture Polymer L-PBF system at the Technical University of Denmark (DTU) by incorporating a fiber laser into a re-engineered Powder Bed Fusion machine, now allowing research for Polymer

Selective Laser Sintering (SLS) materials.

Research in the past has shown that the absorptivity of polymeric materials is very low when attempted to be processed by a fiber laser (1080nm) [1]. Whereas the absorptivity of polymeric materials is much higher when processed with a CO₂ Laser (10,6µm) [1][2][3]. Molecular vibrations of polymeric materials define their optical response to electromagnetic waves at different wavelengths [1]. Organic polymeric materials with aliphatic carbon-hydrogen (C-H) bonds have molecular vibrations in response to electromagnetic waves between 7,5 to 12,5 µm, hence polyamides display high absorptance at 10,6 µm [3]. Since the absorptance for the selected fiber laser is low, most of the energy delivered by the laser is lost in reflectance and transmittance. To improve the absorptance of the powders for CO₂ laser wavelengths, additives such as silicon dioxide (SiO₂) & titanium dioxide (TiO₂) are used for polyamide powders [3]. Similarly, work has been carried out to explore the potential of sintering polymers loaded with carbon black as an optical absorber [4][5]. Similar to carbon black any optical absorber (effective at the 1080nm wavelength) theoretically can assist in the consolidation of the powder layer using a fiber laser. This work will explore the last mentioned effect, and how minimising the amount of optical absorber effects the functional production of SLS parts.

Experimental methods

Two kinds of the same PA11 material were used for the experiments. The materials were characterised prior to mixing and laser sintering. To develop the process parameters used during sample manufacturing the individual powders were characterised by, Differential Scanning Calorimetry (DSC), Thermal Gravimetric Analysis (TGA), and powder sizing. These methods inform important aspects of the manufacturing process, the black optical absorber content, and the mixing reliability.

The materials used are the same type of PA11 from BASF Ultrasint[®]. The major difference is that a black optical absorber is added for the one batch colouring this black. The two materials have previously been processed on the Open polymer L-PBF platform developed at DTU. However, with little success due to either too low or too high absorptivity. To mitigate this the two powders have been mixed. The goal is to achieve the lowest black optical absorber loading possible, to have the lightest grey colour of the final parts. Having a light grey colour will in turn open the possibility for direct manufacturing with coloured plastic powders in L-PBF, or easy dyeing into a desired colour.

DSC analysis has been conducted on both polymer types using the Waters Discovery DSC, to determine the melt and crystallisation temperature. The DSC was done at standard conditions in a nitrogen atmosphere, heating at 10.00°C/min. Heating from 0°C to 230°C, with a subsequent cooling ramp at 10.00°C/min to 0°C. The extracted melting and recrystallisation temperatures have been used for determining the process settings, considering the chamber heating and the final desired melt pool temperature. Based on the DSC curves it was found that the melting temperatures are very close, which is expected to cause the polymers to melt into a homogeneous plastic and not a two-component mix of molten plastic 1 with inclusions of plastic 2. This fully melted plastic part is only expected when the energy absorption in the black part is large enough to obtain and deliver the energy from the laser, onto the white powder, ensuring a fully melted region. The melting and crystallisation temperatures can be seen in Table 1 as well as in Figure 1.

Polymer	Melting (°C)	Crystallisation (°C)
PA11 White	200	159
PA11 Black	200	168

Table 1: DSC results

Based on the results an initial chamber temperature of 185°C was selected, with the top heaters set to 195°C. The resulting temperature for the build job will by these settings be 175°C, as determined by previous experiments [6]. This temperature will ensure that the polymer stays in a molten state and will only crystallise a little before the entire build is done and the machine is set to cool down. The powder cake cools down for a minimum of 12 hours, after which the parts are removed.

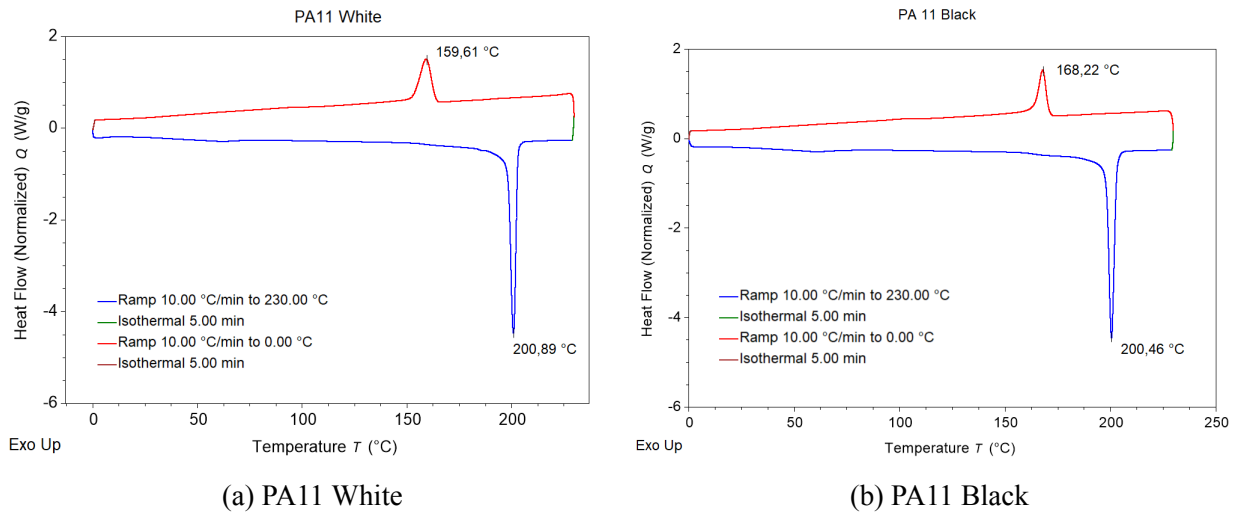


Figure 1: DSC analysis of the two powders used for mixing.

A TGA analysis was carried out to identify the amount of filler in the black PA11 material. It is assumed that the major constituent in the filler is the black optical absorber. The analysis was done on a Waters Discovery TGA showing the composition between the PA11 and filler loading in the powder. The TGA was run at standard conditions in a nitrogen atmosphere, heating the sample at 10°C/min to a final temperature of 800°C. The filler composition has not been explored further since the material is a proprietary blend from BASF.

Figure 2 shows the filler is constituting 6,9wt% and is assumed to be the black part in the polymer blend acting as the optical absorber. Optical absorption of the laser will be aided by the black optical absorber, which even at low filler contents is expected to have a large influence on the final part colour. The test of optical absorption will be determined by the manufacturability of the different batches of powder mixes.

To determine the powder size a Malvern Mastersizer 3000 with the dry dispersion method was used. The powder size will influence the mixing homogeneity and the flow properties of the powders [7]. To ensure that the two powders are alike before mixing separate tests were carried out. The results of the powder sizing can be seen in Table 2.

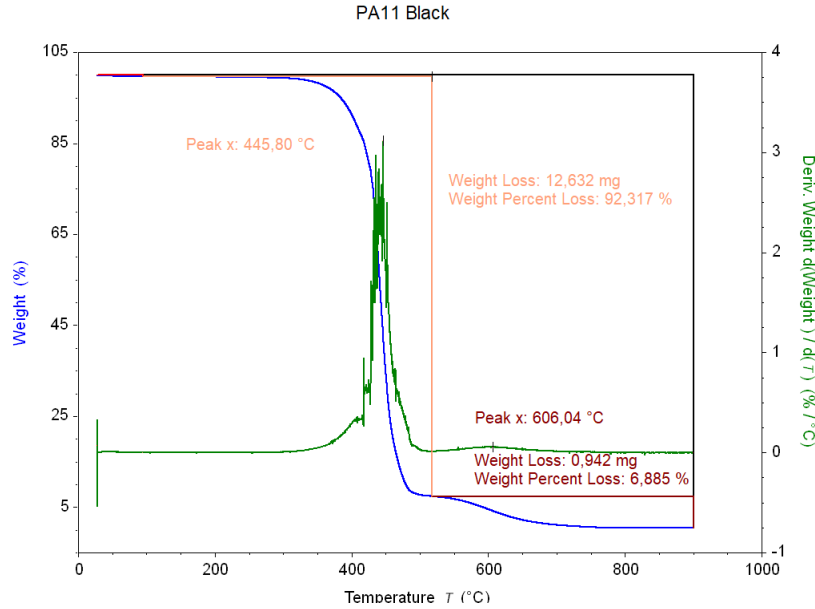


Figure 2: TGA plot for the PA11 Black

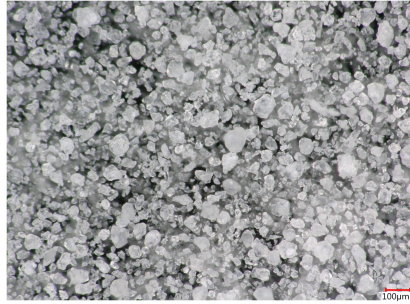
Polymer		PA11 White	PA11 Black
Dv (10)	μm	20,3	23,8
Dv (50)	μm	44,1	46,7
Dv (90)	μm	78,5	79,9
Density (TDS)	kg/m^3	520	540

Table 2: Powder specification and sizing

Three different batches of powder have been produced. The batches are White/Black 50/50, 80/20, and a 95/5 batch. Based on the powder properties a tumble mixer was selected. Tumble mixing is suitable when the powders to be mixed are like each other in size, weight, and particle shape [7]. Considering the densities, and powder size are alike according to Table 2, the only difference can be in the powder morphology. This has been investigated by light optical microscopy as shown in Figure 3. Both powders have the same rough and uneven morphology, likely caused by the manufacturing method. This leads to an expectation of complete random mixing between the two powders. A random mixing will ensure a homogeneous mix throughout the batch. The same mixing routine has been used for all batches.

The mixed powders can be seen in Figure 4. The mixing appears uniform, for all batches, with the white hue intensifying between every batch, ranging from W/B 50/50 to 95/5. Based on these results the mixed powders have been used for process optimisation, part production, and testing.

Mixing the powders result in a smaller amount of the black optical absorber ensuring a lighter colour compared to the 100% black powder. The optical absorber loading will for the batches tested be 3,45%, 1,39%, and 0,35% for the W/B 50/50, 80/20, and 95/5 respectively.

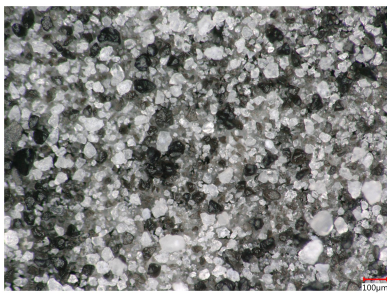


(a) PA11 White morphology

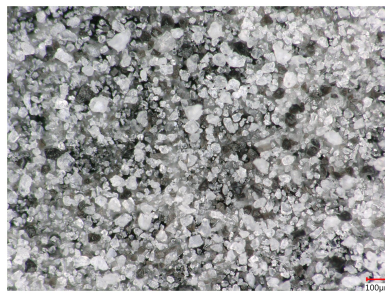


(b) PA11 Black morphology

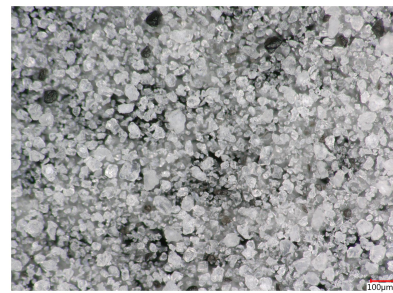
Figure 3: Morphology comparison between the unmixed white and black powder (Keyence optical microscope 200x)



(a) 50/50 W/B morphology



(b) 80/20 W/B morphology



(c) 95/5 W/B morphology

Figure 4: Morphology comparison between the different batches of powder

Test samples were produced on the Open Architecture L-PBF for polymer powders, developed at DTU. The machine is a re-engineered Projet 4500 originally from 3D Systems. The open platform uses the stock powder handling, and build piston axis, with changes to all other subsystems. The machine uses a 300W CW fiber laser source with a 0,2mm spot size [8] to produce the parts. Machine control is achieved by a unified systems controller [9], controlling laser movements and power, as well as the linear motions. Heating for the build chamber is done from all six sides, with heating elements placed on all four sides, and under the build bed, as well as two ceramic heaters placed above the bed. The machine has been developed as a materials investigation platform, challenging the traditional use of CO₂ lasers, by using a fiber laser source. The atmosphere is uncontrolled, causing material degradation, but is not expected to influence the processing capabilities of the machine. The heaters will maintain 180°C in the powder cake build area, ensuring little crystallisation before cool-down. The process is monitored by an infrared camera (Opatrix Xi400), to obtain the build bed temperature and ensure steady process control throughout the build. This is currently controlled by operator input during the run-in of new materials. The recoater is a roller recoater, rolling in the opposite direction of the recoater movement, ensuring good packing and distribution of the powder across the powder bed.

The batches of powder used in the process are new introductions to the Open polymer L-PBF platform. Because of this, all batches have required process optimisation for final part quality. The

process optimisation was done by varying the parameters influencing the energy density of the laser equation 1. Here P is laser power in watts, h is the hatch spacing of the laser scan tracks, s is the scan speed, and l is the layer thickness. Furthermore, the build temperature has been tuned to align with the DSC results.

$$vED = \frac{P}{h \cdot s \cdot l} \quad (1)$$

Several factors influence the final sintering of the powder when varying the energy density. To ensure that complete sintering has been carried out, trials for powder consolidation with different parameter combinations of varying laser power and hatch spacing were assessed.

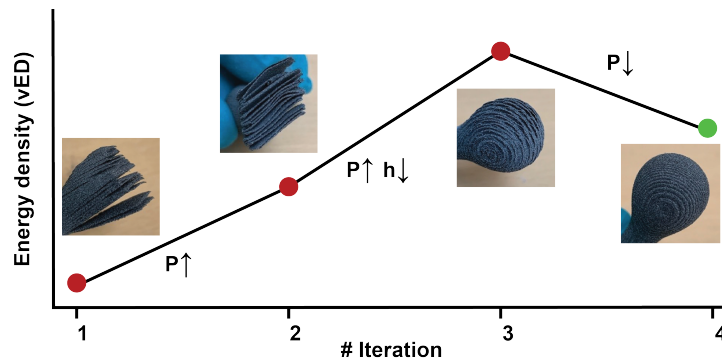


Figure 5: Iterative approach for the process optimisation, here shown for the 50/50 batch

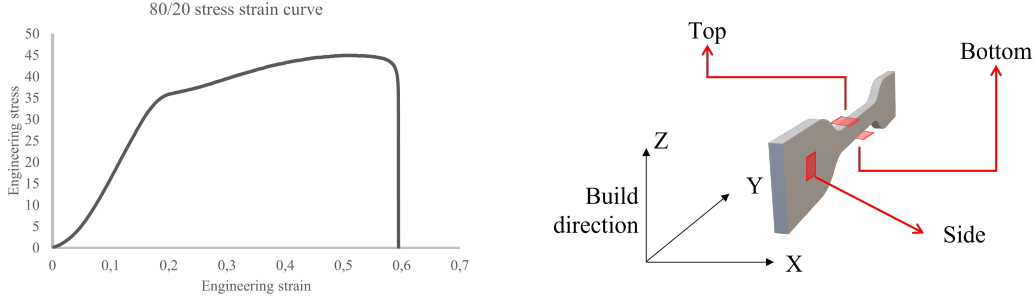
Process optimisation of all batches investigated several different process settings before finding the right fit. Iterative process optimisation was adopted varying the parameters considered by vED . This process allowed for production of parts at different energy densities, and a conclusion based on the build and sintering quality, as seen in Figure 5. The best fit process parameters were the initial settings used for the next batch. From this baseline, a process optimisation was carried out. For all production runs the temperature settings were kept constant, ensuring a build chamber temperature of 180°C and a top bed temperature of 185°C.

Part characterisation

The manufacturability of the batches was initially determined in the first step of the process optimisation. Several different parameters were explored. The assessment of process stability was inferred from; the change of colour during laser processing, measurement of melt temperature, the flatness of the part in the bed, and stable recoating.

To quantify the different manufacturing strategies and compare the batches, tensile tests and surface roughness measurements were carried out on the final parts. The tensile testing specimens were as per ISO 527-2, design type 5A. In total 6 test specimens were manufactured, 5 for mechanical testing and 1 for surface roughness characterisation. The specimens were built such that the largest cross-section area was along the XY plane, see Figure 6b. The tensile test specimen was characterised using a Mecmesin Multitest-i, with a 1000N load cell. A characteristic curve of the tensile testing

is shown in Figure 6a. The tensile testing results are compared to the supplier datasheet values to determine if the part production is successful. Both the surface roughness and tensile test results are compared between the different batches, to check whether the batches with low optical absorber content can produce comparable parts.



(a) Representation of the typical tensile test for the 80/20 batch.

(b) Tensile test specimen, build orientation and surfaces for characterisation.

Figure 6: Tensile curve and the part build orientation, showing the surface roughness measurement locations

The planar surfaces of the tensile test specimens were used to characterise the surface roughness for varying concentrations of the optical absorber. The data was acquired using a focus variation microscope, Alicona InfiniteFocus G4 and was analysed using SPIP™. The inspection was carried out at a single position on each face of the tensile test specimen, see Figure 6b. The data was acquired over an area of 2,85mm x 2,16mm, with a lateral resolution of 2,2µm, and a vertical resolution of 410nm. The data was processed in SPIP™ to correct for the inclination of the component while measuring, and any curvature of the measured surface. The surface roughness was quantified by extracting the areal arithmetic mean height (S_a) as defined in ISO standard 25178-2, see Equation 2.

$$S_a = \frac{1}{A} \iint_{\bar{A}} |z(x, y)| dx dy \quad (2)$$

Results

The initial hypothesis was that lowering the amount of optical absorber would significantly narrow the processing window and produce parts that would show more instabilities and larger deviations considering the mechanical properties. The added expectation was a rougher surface comprised of more adhering particles.

The production of each batch saw a sharp increase in the energy density required for processing the powder. Two parameters from the energy density were kept constant, to allow for variation of the other two. The two constant parameters were the scan speed and the layer thickness. The parameters for each batch including the constant parameters can be seen in Table 3. The scan speed was locked due to limitations of the galvano mirror device, and the controller. While the layer thickness was kept constant, to avoid changes in the material behaviour caused by increasing the

possibility of several powder grains stacked on top of each other. The influence of both scanning speed and layer thickness can be investigated further. The scan tracks were initially determined to benefit from not overlapping. To accommodate this a hatch spacing of $300\mu\text{m}$ was used. This was done to ensure a low enough energy density, since the equipment cannot go low enough in power, and the speed could not be set any higher. This was eventually minimised to match the spot size of the laser, as the energy density requirement was greater for the batches having more white powder. The top temperature was also subject to change when moving from the 50/50 batch to the 80/20. The temperature change was needed due to curling and warping during the initial layers of production, which was induced by the thermal shock of the laser. The temperature was set to 5°C higher than for the previous batch, solving the problem.

		50/50	80/20	95/5
Scan speed	mm/s	3000	3000	3000
Layer thickness	μm	60	60	60
Hatch spacing	μm	300	234	200
Laser power	W	35	35	60
Top temperature	$^\circ\text{C}$	180	185	185
Build temperature	$^\circ\text{C}$	175	175	175

Table 3: Process parameters for the batches of the material tested

An increase in energy density is needed for achieving consolidation of the batches containing small amounts of the optical absorber. The melting and consolidation of the powder were seen to allow the optical absorber to flow out into the entire layer of the part, even when using the 95/5 batch, turning the entire part black internally. The process optimisation proved that sintering powders with a black optical absorber content close to 0,34% are possible while achieving consolidated parts.

When lowering the optical absorber content it is seen that a change in hatch spacing is needed since each black powder particle is spread further apart. A wider hatch spacing with a narrower spot size causes a gap between two scan tracks, which increases the risk of missing a black powder particle completely, causing less energy uptake. The shift is evident between the 50/50 and 80/20 batches, where the same laser power was used, but a significant change in hatch spacing was observed. However, when looking into the parameters of the 95/5 batch the number of black powder particles has been decreased to a point where the chance of hitting a black powder particle (Figure 4) must be optimised. This is done by having the scan tracks adjacent to each other. Processing the 95/5 batch also inferred a large increase in the laser power, due to the low absorptivity of the white powder particles dominating the batch.

The manufactured parts suggest that even lower amounts of the optical absorber can be used when dealing with a fiber laser if the power output and scan speeds can be adjusted accordingly. For the current system, this has not been dealt with further due to the scan speed limitations currently in place. Lowering the optical absorber content could, however, infer that not enough energy is absorbed into the powder, causing the energy to dissipate further into the powder bed. This energy dissipation into the powder bed has previously been seen to cause large instabilities of the desired

geometry of the parts.

Verification of the mechanical properties was used for determining the part quality, in terms of the consolidation between layers, and the overall manufacturing stability. There was a slight deviation between the batches, with the 80/20 batch showing the best mechanical properties. The mechanical properties of the parts are determined by the melt zone and how much the white powder has melted, as well as the layer-to-layer consolidation. Both are controlled by the energy absorption in the powder, as well as the rheological properties. The two constituent powders have not been tested for their rheological properties but are expected to start flowing even though the shear in the process is very low. This flow of the black molten polymer was observed during manufacturing. The flow caused by melting the black powder will allow for it to surround the white particles and provide heat for either melting or fusing them. The results presented in Figure 7 suggest that the 80/20 batch is the best batch produced, providing good mechanical properties even, when compared to the datasheet values from the supplier. This is contributed to the flow and relatively high content of the black particles in the mix, allowing for proper melting of the parts during production.

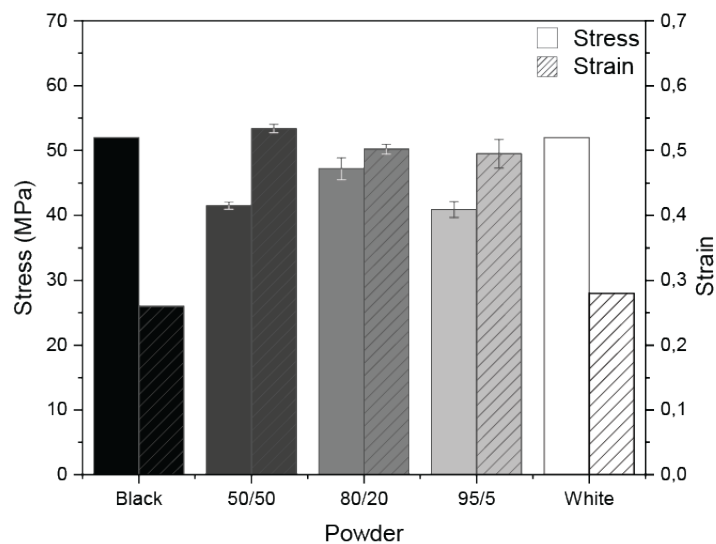


Figure 7: Engineering Stress and strain results for varying Black to White powder ratio concerning supplier datasheet (White Black)

The parts produced from the 95/5 batch showed comparable results to those of the 50/50 batch, leading to the conclusion that even lower optical absorber levels could be used to produce parts. These parts would be expected to show comparable, if not slightly lower mechanical properties, but at a much lighter grey colour. The strain results from the tensile tests proved that the parts behave differently from the datasheet values. The deviation in mechanical properties is attributed to the machine used for production not having an inert and dry atmosphere during manufacturing, causing moisture uptake in the manufactured parts. The moisture ingress during the manufacturing process cannot be avoided due to the limitations of the current machine setup. This moisture uptake will for PA11 cause a hydrolysing effect, leading to chain scission and a change in both the tensile

strain and strength [10][11]. This effect can also be the influencing factor, as to why the stress levels for the manufactured parts were lower than the datasheet values found. The effect of the optical absorber content on mechanical properties is still unexplored.

The surface roughness, Sa, characterised for the varying mixing ratios of black to white powder is shown in Figure 8. From the three faces characterised, the surface roughness for the XZ plane (vertical) was found to be the highest. This can be attributed to the caterpillar effect which can be a function of the layers and the layerwise scan track rotation. The waviness profile of the caterpillaring effect (see Figure 9a & 9d) has a period of 300µm which is equivalent to 5 layers of 60µm each, i.e. every 6 layers there is a formation of the bulge in the lateral dimension. This can be mitigated by optimizing with contour process parameters for the individual mixtures.

The surface roughness for the top and bottom surface was significantly better as the scan tracks would bring the entire layer to a melt. Even though the bottom face was built on the powder bed directly, it is almost equivalent to that of top face. The almost similar Sa values are representative of well identified process parameters for the mixtures used.

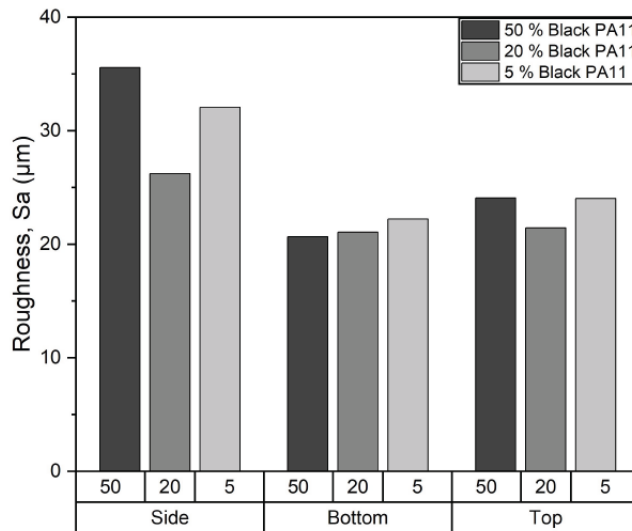


Figure 8: Surface roughness, Sa, for varying mixing ratios

Just like the powder particles being stuck in the black molten matrix discussed above, the surface roughness is also typically caused by powder particles sticking to the side of the parts. These powder particles are not fully molten due to too low energy but will adhere to the surface of the underlying molten matrix, typically causing the surface roughness to be a function of the size of these powder particles.

The 80/20 batch overall had the most uniform surface roughness. The comparison of areal plots between the 80/20 to the 95/5 batch can be observed in Figure 9. The side faces for both show the caterpillaring effect (in the form of lines along X in the XY plane) mentioned above. In general, when comparing all three faces, it is evident that the texture of the faces is relatively the same with the difference being that the 95/5 mix consists of more satellite powder particles sintered along the walls. The results presented are comparable to that of industrially manufactured and post-processed

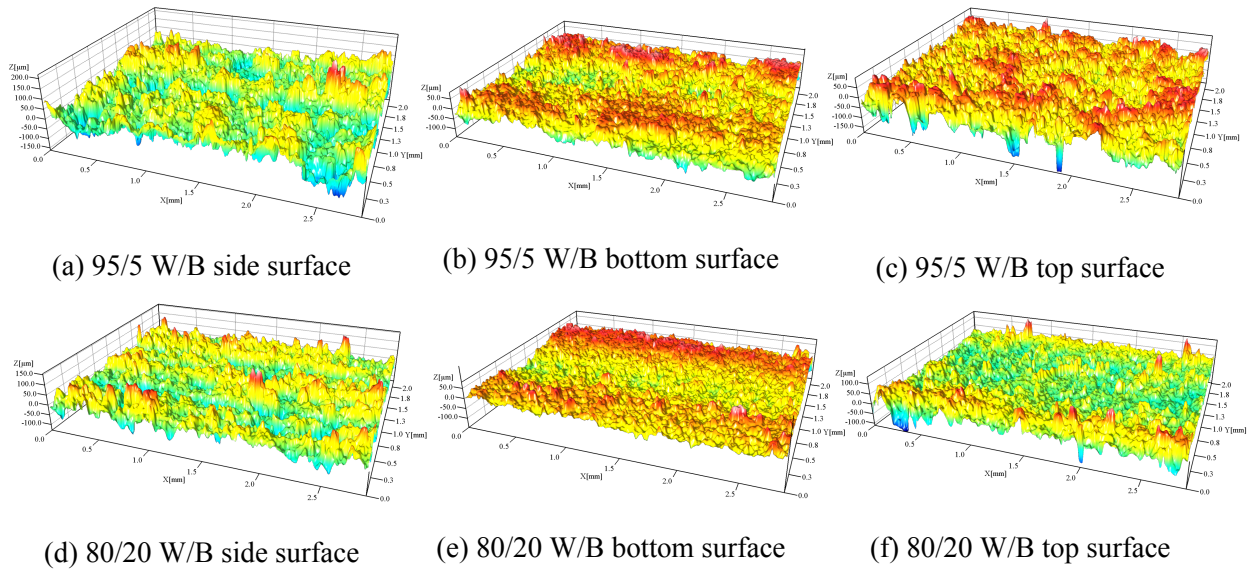


Figure 9: Surface comparison of parts with lower content optical absorber

PA12 SLS parts [12]. To process the 95/5 batch the laser power (effectively the energy density) was scaled up to compensate for the low optical absorber content, hence possibly dissipating more energy along the walls. Indicating the need for a further study into optimising the parameters and identifying the benefits/losses in functionality going lower or higher in optical absorber content.

Conclusion

Several ratios of white and black powder were mixed and manufactured successfully on the Open Architecture Polymer L-PBF system developed at DTU. All the batches processed showed mechanical properties comparable to the supplier data sheets. Reducing the optical absorber (as a function of the mixing ratio) was successful considering the manufacturing of parts. The parts produced showed both mechanical and surface roughness characteristics comparable to results found in the literature. The conclusion is therefore two-fold; 1. The batch processed to the highest quality by the measures in this investigation was the 80/20 mix. 2. Depending on the final part requirement it is possible to go as low as 0,34% optical absorber while producing parts with good surface finish, and functional mechanical properties. The study proved that it is feasible to manufacture parts with low amounts of optical absorber while using a fiber laser at 1080nm wavelength. The investigation was carried out in an uncontrolled atmosphere, and for future work, it is desired to test the capabilities in a controlled N₂ atmosphere, as well as the influence on the final part properties. The current hue of the parts shows potential for post-colouring. The study suggests that optical absorber content can be lowered further, however, this can lead to detrimental effects of over-sintering the parts. By lowering the optical absorber content further, it will be possible to achieve lighter colours when developing the process. To make a precise estimate of by how much to reduce the optical absorber content, the optical properties of both black and white PA11 powder will be characterized for the near-infrared wavelength and its role in the consolidation mechanics will be explored in the future work.

References

- [1] Nikolay K Tolochko et al. “Absorptance of powder materials suitable for laser sintering”. In: (). URL: http://www.mcbuf.com/research_registers/aa.asp.
- [2] J. P. Kruth et al. “Lasers and materials in selective laser sintering”. In: *Assembly Automation* 23.4 (2003), pp. 357–371. ISSN: 01445154. DOI: [10.1108/01445150310698652](https://doi.org/10.1108/01445150310698652).
- [3] Manfred Schmid. “LS Materials: Polymer Properties”. In: *Laser Sintering with Plastics* (2018), pp. 65–99. DOI: [10.3139/9781569906842.004](https://doi.org/10.3139/9781569906842.004).
- [4] Siddharth Ram Athreya, Kyriaki Kalaitzidou, and Suman Das. “Processing and characterization of a carbon black-filled electrically conductive Nylon-12 nanocomposite produced by selective laser sintering”. In: *Materials Science and Engineering A* 527.10-11 (2010), pp. 2637–2642. ISSN: 09215093. DOI: [10.1016/j.msea.2009.12.028](https://doi.org/10.1016/j.msea.2009.12.028). URL: <http://dx.doi.org/10.1016/j.msea.2009.12.028>.
- [5] N. Woicke, T. Wagner, and P. Eyerer. “Carbon assisted laser sintering of thermoplastic polymers”. In: *Annual Technical Conference - ANTEC, Conference Proceedings* 7.January 2005 (2005), pp. 36–40.
- [6] Christian L Budden et al. “Chamber Heat Calibration by Emissivity Measurements in an Open Source SLS System”. In: *Summer Topical Meeting: Advancing Precision in Additive Manufacturing - ASPE-euspen, conference proceedings*. 2022.
- [7] Martin J Rhodes. *Principles of powder technology*. Wiley, 1990, XI, 439 S (unknown). ISBN: 0471924229, 9780471924227.
- [8] MaxPhotonics. *MAXMaxphotonics Co.,Ltd*. URL: <http://en.maxphotonics.com/product/18.html>.
- [9] Sebastian Aagaard Andersen. *Open Architecture Laser Power Bed Additive Manufacturing*. 2020.
- [10] John Moalli, Society of Plastics Engineers, and N Y Plastics Design Library Norwich. *Plastics failure : analysis and prevention*. Ed. by John Moalli. Plastics Design Library, 2001, Online–Ressource (IV, 341 S) (unknown). ISBN: 008095054x, 081551865X, 081551865x, 1282011391, 1591242509, 1884207928, 9780080950549, 9780815518655, 9781282011397, 9781591242505, 9781884207921.
- [11] Pierre Yves Le Gac et al. “Yield stress changes induced by water in polyamide 6: Characterization and modeling”. In: *Polymer Degradation and Stability* 137 (2017), pp. 272–280. ISSN: 18732321, 01413910. DOI: [10.1016/j.polymerdegradstab.2017.02.003](https://doi.org/10.1016/j.polymerdegradstab.2017.02.003).
- [12] M. Launhardt et al. “Detecting surface roughness on SLS parts with various measuring techniques”. In: *Polymer Testing* 53 (Aug. 2016), pp. 217–226. ISSN: 01429418. DOI: [10.1016/J.POLYMERTESTING.2016.05.022](https://doi.org/10.1016/J.POLYMERTESTING.2016.05.022).